Theoretical Study of the Oxidative Addition of 16-Electron d^4 [*n*]-Metallocenophane Complexes with Methane

Ming-Der Su*,† and San-Yan Chu*,‡

Department of Chemistry, National Tsing Hua University, Hsinchu 30043, Taiwan, ROC, and School of Chemistry, Kaohsiung Medical University, Kaohsiung 80708, Taiwan, ROC

Received: August 23, 2000; In Final Form: November 21, 2000

We have chosen eight [*n*]-metallocenophane complexes to investigate the oxidative additions with methane using the B3LYP/LANL2DZ level of theory. Considering the effects from the geometry and the nature of the metal center, the following conclusions emerge: the less bent 16-electron [*n*]-metallocenophane complex with the transition metal center W should be a potential model for the oxidative addition of saturated C−H bonds. Our model calculations suggest that a methane σ-complex intermediate formed between the [*n*]-metallocenophane and methane plays a major role in the oxidative additions. Moreover, we show that both electronic and geometric effects play a significant role in determining the energy barriers.

I. Introduction

Theoretical and computational studies of the activation of unreactive carbon−hydrogen bonds have attracted great attention ever since the first demonstration of the intermolecular oxidative addition of alkane C−H bonds to transition-metal centers.[1] In a continuing effort to explore the nature of the activation process in the past two decades,[2,3] the unsaturated transition-metal fragments of different structural types have been the subjects of numerous quantum chemical calculations, employing theoretical models ranging from, for example, semiempirical methods[4] and various ab initio techniques[5] to density functional theory.[6] The results of these calculations provide excellent, qualitative accounts for a large range of experimentally observed properties.[7] In fact, we have gained a great deal of insight into the complex nature of the electronic structures of these complicated molecular systems, and qualitative explanations and predictions are found to be very reliable.

Recently, there has been considerable commercial interest in ansa-bridged metallocene complexes[8,9] due to their use in the catalysis of stereoregular olefin polymerization reactions.[10] On a more fundamental level, several groups have reported ansa-bridged metallocene complexes which show interesting changes in structure or reactivity compared to the corresponding unbridged metallocene complexes.[11,12] Green and co-workers have investigated the influence of the ansa bridge on several group 6 metallocene complexes and have noted dramatic reactivity differences in comparison to the unbridged analogues.[8] For example, photolysis of $Cp_2W(H)CH_3$ under matrix isolation conditions has been found to generate tungstenocene (Cp_2W),[13] and Green and co-workers had reported that, upon thermolysis in solution, $Cp_2W(H)CH_3$ generated a species capable of reacting with aromatic C−H bonds.[14−16] In contrast, the ansa-bridged analogue $W[(\eta^5\text{-}C_5H_4)_2CMe_2]H_2$ is photochemically inert.[15]

By analogy to the well-known chemistry of photogenerated tungstenocene,[11,13] an interesting chemistry for the ansa-bridged tungstenocene can be anticipated. At first sight, it seems that the relative reactivity of these 16-electron fragments can be explained on the basis of conventional molecular orbital (MO) theory.[17] In a parallel sandwich Cp_2W complex, the HOMO (see details below) is sheltered between the two Cp rings. On the contrary, when tungstenocene is preorganized into a bent state by linking the two Cp rings with an ansa bridge, its HOMO extends into space, apparently more appropriately oriented for oxidative addition to C−H bonds. In other words, a bent geometry may allow more facile oxidative additions to the C−H bonds of an alkane than the parallel ring structure. Besides this, according to Labella, Chernega, and Green's work,[12] it was suggested that the driving force for elimination reaction in these group 6 metallocene derivatives is the existence of the favored parallel ring structure for the d^4 configuration metallocene. Similar experimental evidence and conclusions can also be found in Green's work.[11] However, there is as far as we know no experimental evidence that parallel ring metallocenes are more reactive to oxidative addition than bent ones.

This paradox aroused our interest to investigate the potential energy surfaces of such reactions using density functional theory (DFT). A study of the important C−H activation reaction, eq 1, was thus undertaken:

$$[n]\text{-metallocenophane} + H{-}CH_3 \rightarrow [n]\text{-metallocenophane(H)(CH}_3) \quad (1)$$

The [*n*]-metallocenophanes studied are $M(\eta^5\text{-}C_5H_5)_2$, [1]-$M(\eta^5\text{-}C_5H_4)_2CH_2$, [2]-$M(\eta^5\text{-}C_5H_5)_2C_2H_4$, and [3]-$M(\eta^5\text{-}C_5H_5)_2SC_2H_4$, where M = Mo and W, as shown in **1**. Also, the most relevant geometrical parameter (θ) for these complexes is defined in **1** (i.e., the cp−M−cp angle; cp = centroids of the Cp ring).

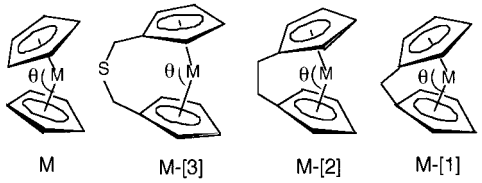

1

† Kaoshiung Medical University.
‡ National Tsing Hua University.

10.1021/jp003037e CCC: $20.00
Published on Web 03/17/2001

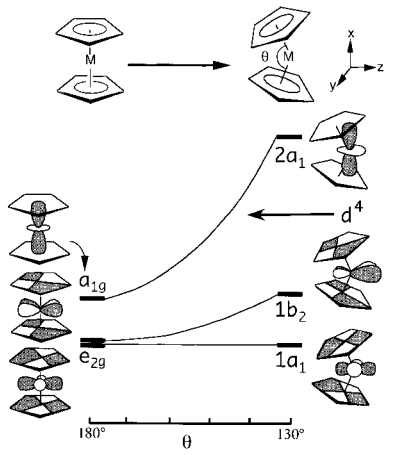

Figure 1. Walsh diagram for bending back the Cp rings in the Cp_2M fragment.

The reasons for choosing eq 1 as the model are the following: (i) Many theoretical studies have been performed on a C−H oxidative addition to Rh, Ir, Pd, and Pt organometallic species.[3−7] However, only a few have actually been carried out on oxidative additions by other transition-metal complexes. Especially little is known about how much the C−H oxidative addition is influenced by Mo and W metals. (ii) To the best of our knowledge, there are no systematic theoretical calculations concerning geometrical effects on the 16-electron d^4 [*n*]-metallocenophane systems.[18,19] In the present work, we thus use the number of bridging atoms to adjust the bending angle θ. As will be shown later, θ decreases along the series, M(η^5-$C_5H_5)_2$, [3]-M(η^5-$C_5H_5)_2SC_2H_4$, [2]-M(η^5-$C_5H_5)_2C_2H_4$, and [1]-M(η^5-$C_5H_4)_2CH_2$, as expected. Through this theoretical study, we hope (a) to obtain a detailed understanding of the C−H oxidative addition to 16-electron d^4 [*n*]-metallocenophane type complexes, (b) to investigate the influence of the ansa bridge upon the geometries and energies of the intermediates, as well as on the transition states, (c) to elucidate the differences between Mo and W, and (d) to investigate those factors controlling the activation barrier for oxidative reactions. It will be shown that the reactivity of the 16-electron d^4 [*n*]-metallocenophane complex is correlated strongly to its singlet−triplet splitting.

II. Electronic Structure of [*n*]-Metallocenophane + CH_4

It is convenient to divide the reactants into d^4 C_{2v} Cp_2M and CH_4 fragments and begin a discussion of the bonding by looking briefly at the valence orbitals of the Cp_2M and CH_4 units. The orbitals of the Cp_2M fragment are known and have been studied extensively by Hoffmann et al.[17,20] and Ziegler et al.[21] using different approaches. Figure 1 shows a qualitative Walsh diagram for changing the bending angle θ. The d^4 Cp_2M fragment has three characteristic frontier orbitals, $1a_1(d_{y^2-z^2})$, $1b_2(d_{yz})$, and $2a_1(d_{z^2})$, which are primarily metal d orbitals. It should be emphasized here that some metal $d_{y^2-z^2}$ and s characters from $1a_1$ mix into $2a_1$ so that the torus of d_{z^2} becomes hybridized away from the Cp ligands.

III. Geometries and Energetics of [*n*]-Metallocenophane + CH_4

In this section the computational results for four regions on the potential energy surfaces will be presented: 16-electron [*n*]-metallocenophane plus free CH_4 (**Rea**); a precursor complex (**PC**); the transition state (**TS**); the oxidative addition product (**Pro**) [*n*]-metallocenophane(H)(CH_3). The fully optimized geometries for those stationary points calculated at the B3LYP/LANL2DZ level are given in Figures 2−5, respectively. Total and relative energies are collected in Table 1.

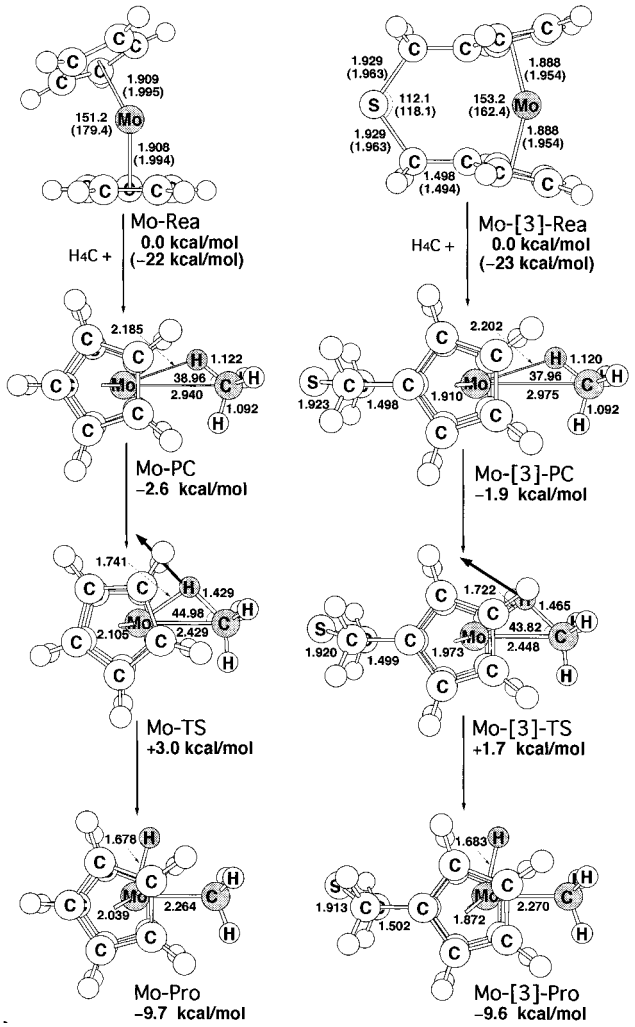

Figure 2. B3LYP/LANL2DZ optimized geometries (in Å and deg) of the reactants (singlet and triplet), precursor complex, transition state, and product of **Mo-[3]** and **Mo** cases. Values in parentheses are at the triplet state. The heavy arrows indicate the main atomic motions in the transition state eigenvector.

(A) Reactant. A general outline of the valence MOs in the bent metallocene has been given in section II. Reactants **Mo-Rea**-**Mo-[3]-Rea** and **W-Rea**-**W-[3]-Rea** have been calculated both as low-spin (singlet) and as high-spin (triplet) complexes. As expected, no matter what multiplicity the bent metallocene adopts, our computations suggest that the bending angle θ should always decrease in the following order: **Mo-[3]-Rea** > **Mo**−**Rea** > **Mo-[2]-Rea** > **Mo-[1]-Rea** and **W-[3]-Rea** > **W-Rea** > **W-[2]-Rea** > **W-[1]-Rea**. Additionally, our DFT calculations indicate that they all possess a triplet ground state. As one can see in Figure 1, for a high-spin d^4 complex, configuration $(1a_1)^2$-$(1b_2)^1(2a_1)^1$, the Walsh diagram predicts that a parallel ring structure is preferred, which has been confirmed by some experimental observations.[13] For instance, infrared and UV matrix-isolation studies[13b] have shown Cp_2W to have a parallel sandwich structure with a $^3E_2$ ground state. On the basis of these results, it is therefore expected that the singlet state of the d^4 Cp_2M system should be more bent than its triplet analogue. This prediction agrees well with our B3LYP/LANL2DZ results for all cases as shown in Figures 2−5. Our theoretical results for

TABLE 1: Relative Energies for Singlet and Triplet [*n*]-Metallocenophane Fragments and for the Process [*n*]-Metallocenophane + H−CH_3 → Precursor Complex → Transition State → Product[a]

systems	θ (Cp−M−Cp) (deg)	ΔE_{st}[b] (kcal/mol)	reactant (kcal/mol)	ΔE_{cpx}[c] (kcal/mol)	ΔE_{act}[d] (kcal/mol)	ΔE[e] (kcal/mol)
Mo	151.2	−22.6	0	−2.55	+2.95	−9.65
Mo-[3]	153.2	−23.1	0	−1.86	+1.74	−9.58
Mo-[2]	139.2	−9.15	0	−3.48	+6.65	−6.66
Mo-[1]	125.8	−4.64	0	−4.52	+7.90	−5.11
W	154.9	−18.9	0	−4.70	−0.278	−23.7
W-[3]	161.7	−19.4	0	−7.57	−3.80	−26.4
W-[2]	140.7	−7.76	0	−1.61	+4.25	−22.4
W-[1]	126.9	−5.17	0	−1.28	+4.21	−22.1

[a] At the B3LYP/LANL2DZ level. [b] $\Delta E_{st} = E_{triplet} - E_{singlet}$. A negative value means the triplet is the ground state. [c] The stabilization energy of the precursor complex, relative to the corresponding reactants. [d] The activation energy of the transition state, relative to the corresponding reactants. [e] The exothermicity of the product, relative to the corresponding reactants.

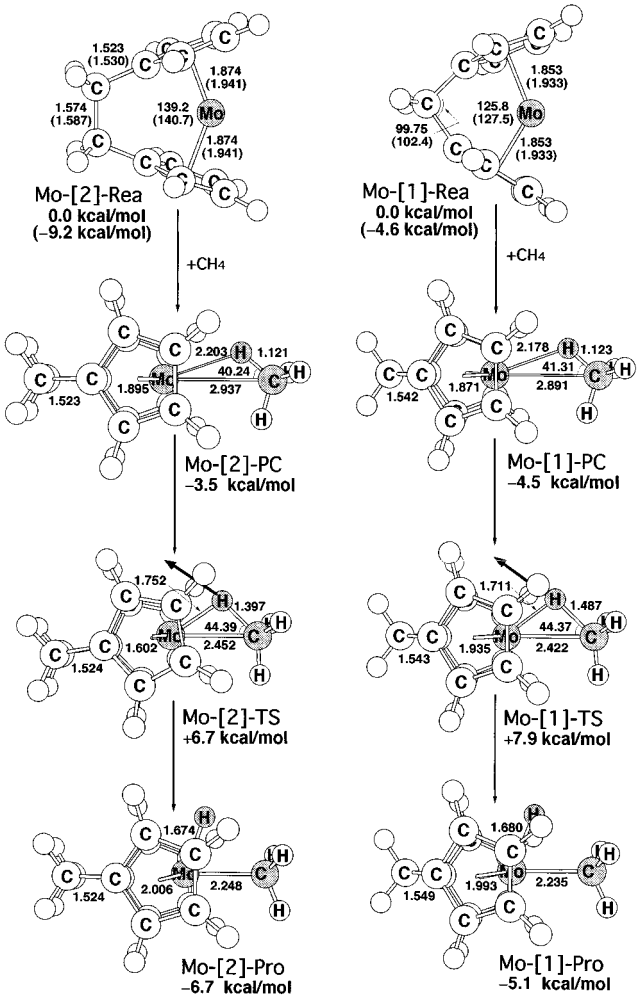

Figure 3. B3LYP/LANL2DZ optimized geometries (in Å and deg) of the reactants (singlet and triplet), precursor complex, transition state, and product of **Mo-[1]** and **Mo-[2]** cases. Values in parentheses are at the triplet state. The heavy arrows indicate the main atomic motions in the transition state eigenvector.

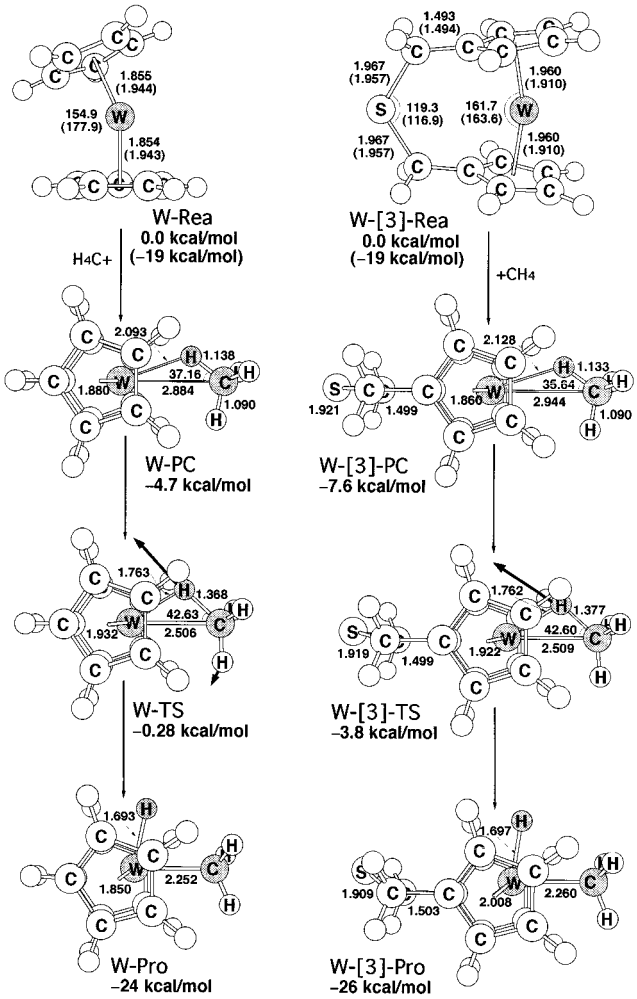

Figure 4. B3LYP/LANL2DZ optimized geometries (in Å and deg) of the reactants (singlet and triplet), precursor complex, transition state, and product of **W-[3]** and **W** cases. Values in parentheses are at the triplet state. The heavy arrows indicate the main atomic motions in the transition state eigenvector.

singlet metallocene preferring the bent structure are also consistent with those of Green and Jardine.[15]

Moreover, in a bent geometry at the singlet state, the HOMO ($1b_2$) is destabilized as the bending angle θ decreases and the LUMO ($2a_1$) increases in energy, resulting in an opening of a HOMO−LUMO gap in the bent d^4 Cp_2M complex. In other words, the energy gap between the HOMO and LUMO levels for the d^4 Cp_2M singlet species is strongly dependent on the bending angle θ as shown in Figure 1; i.e., the larger the bending angle θ, the smaller (i.e., the more negative) the singlet−triplet splitting ($\Delta E_{st} = E_{triplet} - E_{singlet}$) of the d^4 Cp_2M complex. Our DFT results are in accord with this prediction. That is to say, the magnitude of the singlet−triplet splitting of the bent metallocene reactant follows the same trend as the bending angle θ: **Mo-[3]-Rea** (−23.6 kcal/mol) < **Mo−Rea** (−23.1 kcal/mol) < **Mo-[2]-Rea** (−9.15 kcal/mol) < **Mo-[1]-Rea** (−4.64 kcal/mol) and **W-[3]-Rea** (−19.4 kcal/mol) < **W-Rea** (−18.9 kcal/mol) < **W-[2]-Rea** (−7.76 kcal/mol) < **W-[1]-Rea** (−5.16 kcal/mol). We shall use the above results to explain the origin of barrier heights for their oxidative additions in a latter section.

Furthermore, since the B3LYP/LANL2DZ calculations suggest that these [*n*]-metallocenophane reactants should adopt a

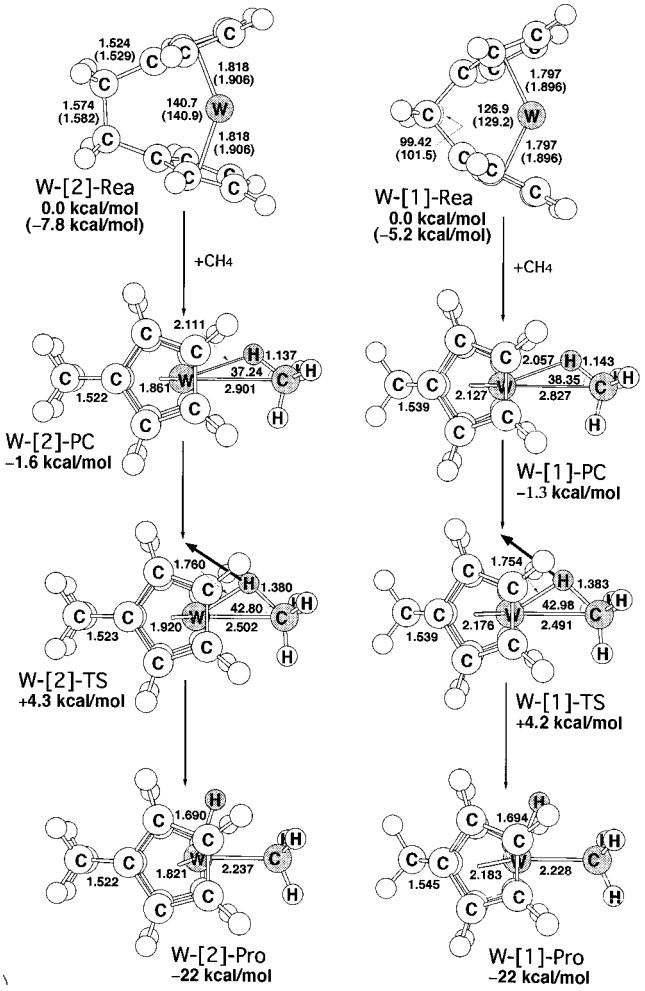

Figure 5. B3LYP/LANL2DZ optimized geometries (in Å and deg) of the reactants (singlet and triplet), precursor complex, transition state, and product of **W-[1]** and **W-[2]** cases. Values in parentheses are at the triplet state. The heavy arrows indicate the main atomic motions in the transition state eigenvector.

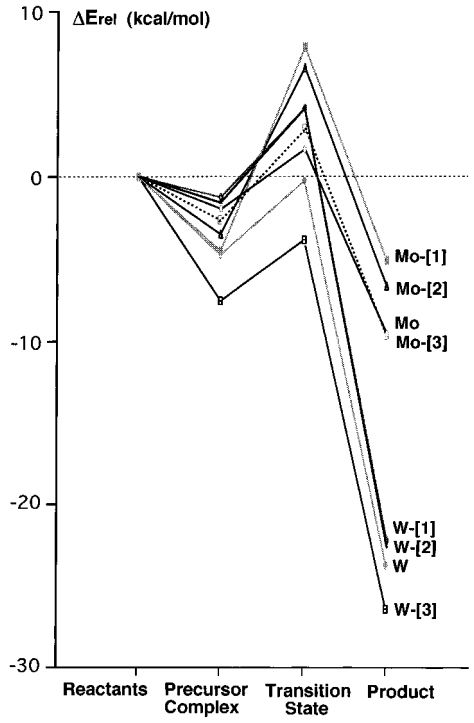

Figure 6. Potential energy profile of the reaction of [*n*]-metallocenophane with CH_4. All of the energies were calculated at the B3LYP/LANL2DZ level. See the text.

triplet ground state, this implies that these complexes might insert into the saturated C−H bond via a diradical-type mechanism. Nevertheless, it is well established that whenever a reactant contains a heavy atom center, which is not necessarily directly involved in the reaction, a strong spin−orbit coupling (SOC) may occur.[22,23] In other words, a triplet reactant, via the agency of the heavy atom, can undergo a spin-inversion process for transformation to the singlet reactant and then proceed along the singlet reaction. In addition, our DFT results in Table 1 also suggested that those reactants with the triplet ground state would have a small excitation energy to the first singlet state; i.e., $\Delta E_{st} = -23 - -4.6$ kcal/mol. Thus, due to the fact that [*n*]-metallocenophane has a small singlet−triplet splitting ΔE_{st} and a heavier transition metal involved, and the SOC is expected to be substantial in those oxidative additions and would wash out differentials based on singlet, triplet distinctions. For these reasons, it could well be that the oxidative addition reactions proceed on the singlet surface, even if the reactants start from the triplet state. We shall therefore focus on the singlet surface from now on.[24]

(B) Precursor Complex. The structures of precursor complexes (**Mo-[3]-PC**, **Mo-PC**, **Mo-[2]-PC**, **Mo-[1]-PC**, **W-[3]-PC**, **W-PC**, **W-[2]-PC**, and **W-[1]-PC**) optimized at the B3LYP/LANL2DZ level are shown in Figures 3−6, respectively. All the precursor complexes display similar [*n*]-metallocenophane•••(CH_4) bonding characteristics. The methane ligand is coordinated to the metal center in an η^3 fashion via two C−H σ bonds with the H−C−H plane nearly orthogonal to the Cp-M-Cp coordination plane. Calculated vibrational frequencies for the precursor complexes reveal that these structures are true minima on the potential energy surface. Moreover, as shown in Figures 2−5, the M−C distances to CH_4 in these precursor complexes range from 2.98 to 2.83 Å. Such large bond distances between [*n*]-metallocenophane and methane are expected to be reflected in small values for the complex stabilization energy. Indeed, it was estimated that the energy of the precursor complex relative to its corresponding reactants is 1.3−7.6 kcal/mol as shown in Table 1. Hence, it seems that experimental detection of intermediates formed in the gas-phase at room temperature is challenging.

(C) Transition State. The optimized transition state structures (**Mo-TS**, **Mo-[3]-TS**, **Mo-[2]-TS**, **Mo-[1]-TS**, **W-TS**, **W-[3]-TS**, **W-[2]-TS**, and **W-[1]-TS**) together with arrows indicating the main atom motion in the transition state eigenvector are shown in Figures 2−5, respectively. All these transition state structures show the same three-center pattern involving metal, carbon, and hydrogen atoms. The transition state vectors represented by the heavy arrows in the transition state structures all are in accordance with the insertion process, primarily the C−H bond stretching with a hydrogen migrating to the metal center. It is noted that such characteristic three-center transition states have been observed in oxidative additions of C−H bonds to 16-electron $CpML_2$[24] and $CpML$[25] and to 14-electron ML_3[26] and ML_2[27] systems.

Furthermore, as seen in Table 1, the energies of both **W-TS** and **W-[3]-TS** transition states for methane insertion are below those of their corresponding reactants. This indicates that the rearrangement shown in **2** can take place without the dissociation of methane from the W(η^5-C_5H_5)$_2$ and [3]-W(η^5-C_5H_5)$_2$$SC_2H_4$ fragments. Consequently, the intermediate η^3-complex we found in this work may correspond to the methane σ complex proposed by Norton et al.[28] and Bercaw et al.[29] Moreover, as shown in

Figure 4, our DFT calculations suggest that the W agostic complex (**W-PC** and **W-[3]-PC**) should be a structure in which methane is bound in an end-on fashion through two hydrogen atoms, which is again in accordance with the mechanism postulated by Norton et al.[28] and Bercaw et al.[29] For these reasons, our theoretical results provide strong support for the existence of alkane "σ-complex" intermediates, which intervene in the saturated hydrocarbon oxidative addition process before full C−H bond cleavage occurs. A similar theoretical calculation of such exchange reactions is also reported by Green and Jardine.[15]

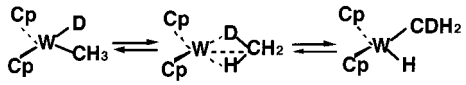

2

(D) Product. The optimized product geometries (**Mo-Pro**, **Mo-[3]-Pro**, Mo-[2]-Pro, **Mo-[1]-Pro**, **W-Pro**, **W-[3]-Pro**, **W-[2]-Pro**, and **W-[1]-Pro**) are also collected in Figures 2−5, respectively. With examination of these product conformations, it is obvious that the methane fragment (H···CH_3) is poised in a fashion consistent with the transition states. Thus, the reaction trajectory for C−H insertion appears to be set in motion into the final product.

IV. Discussion of the Potential Energy Surfaces

The potential energy profiles based on the data in Table 1 are summarized in Figure 6. Four intriguing results can be drawn from this figure.

First, considering the geometrical effect, our theoretical findings suggest that, for the same metal center, complexes containing less bent sandwich structures are considerably more reactive. Namely, this may lead to the lower activation energy and the larger exothermicity for the oxidative addition of H−CH_3 to 16-electron [*n*]-metallocenophane complexes (left to right in Figure 6). For instance, as demonstrated in Table 1, the barrier height for H−CH_3 activation increases in the following order: M = Mo, **Mo-[3]-TS** (3.60 kcal/mol) < **Mo-TS** (5.50 kcal/mol) < **Mo-[2]-TS** (10.1 kcal/mol) < **Mo-[1]-TS** (12.4 kcal/mol); M = W, **W-[3]-TS** (3.77 kcal/mol) < **W-TS** (4.42 kcal/mol) < **W-[1]-TS** (4.49 kcal/mol) < **W-[2]-TS** (5.86 kcal/mol). It should be noted that the activation barriers for the W reactions are generally smaller than those for their Mo analogues.

Second, as shown in Table 1, all the oxidative addition reactions are thermodynamically exothermic. The order of exothermicity follows a similar trend to the activation energy: M = Mo, **Mo-Pro** (−9.65 kcal/mol) < **Mo-[3]-Pro** (−9.58 kcal/mol) < **Mo-[2]-Pro** (−6.66 kcal/mol) < **Mo-[1]-Pro** (−5.11 kcal/mol); M = W, **W-[3]-Pro** (−26.4 kcal/mol) < **W−Pro** (−23.7 kcal/mol) < **W-[1]-Pro** (−22.4 kcal/mol) < **W-[2]-Pro** (−22.1 kcal/mol). Again, it is obvious to see that the W reactions are much more exothermic than their Mo counterparts.

Third, consider the reverse process, that is, the reductive elimination from the alkyl hydride for the [*n*]-metallocenophane species (right to left in Figure 6). Our computational results indicate that the driving force for reductive elimination in these group 6 metallocene derivatives is the formation of the favored parallel ring structure for the d^4 configuration metallocene product. For instance, the activation energy for CH_4 elimination increases in the following order: **Mo-[3]-TS** (11.3 kcal/mol) < **Mo-TS** (12.6 kcal/mol) < **Mo-[1]-TS** (13.0 kcal/mol) < **Mo-[2]-TS** (13.3 kcal/mol); **W-[3]-TS** (22.6 kcal/mol) < **W-TS** (23.4 kcal/mol) < **W-[2]-TS** (23.6 kcal/mol) < **W-[1]-TS** (26.3 kcal/mol). Note that the barriers to reductive elimination for W systems are apparently much higher in energy than those for Mo analogues. Basically, these computational results are qualitatively consistent with some experimental observations.[10−15] For example, it was experimentally found that W(η^5-C_5H_5)$_2$-MeH thermally eliminates methane at 60°, whereas W[(η^5-C_5H_4)$_2$$CMe_2$]MeH is thermally stable at 110°.[10]

Fourth, the DFT results show that the reductive elimination of methane from [*n*]-metallocenophane may proceed through the reversible formation of a methane σ complex, in particular for the [3]-W(η^5-C_5H_5)$_2$$SC_2H_4$ and Mo(η^5-C_5H_5)$_2$ species. Our model calculations are in accordance with some experimental findings.[28,29] For instance, Norton and co-workers had reported that the reversible formation of a σ complex of methane as an intermediate in the elimination process is the most plausible explanation for the H/CH_3 scrambling and for the inverse isotope effect.[28]

V. Theoretical Model for the Reaction Barrier

In this section, an interesting model for interpreting the reactivity of oxidative addition reactions is provided by the so-called configuration mixing (CM) model, which is based on Pross and Shaik's work.[30,31] According to the conclusions of this model, the energy barriers governing processes as well as the reaction enthalpies should be proportional to the energy gap ΔE_{st} ($=E_{triplet} - E_{singlet}$) between the singlet and the triplet states of 16-electron [*n*]-metallocenophane complex. In other words, the smaller the ΔE_{st} of [*n*]-metallocenophane, the lower the barrier height and the larger the exothermicity and, in turn, the faster the oxidative addition reaction.

Bearing the above conclusion in mind, we shall explain the origin of the observed trends as shown previously in the following discussion:

(a) Why is the oxidative addition reaction of [*n*]*-metallocenophane with parallel ring structure more facile than that of bent sandwich complex?*

The reason for this can be traced back to the singlet−triplet gap (ΔE_{st}) of 16-electron [*n*]-metallocenophane. It was found that a bent sandwich complex should result in a larger singlet−triplet energy gap than a parallel ring one due to the MO analysis as discussed earlier. From Figures 2−5, it is obvious that the bending angle θ decreases in the order **Mo-[3]-Rea** > **Mo-Rea** > **Mo-[2]-Rea** > **Mo-[1]-Rea** and **W-[3]-Rea** > **W-Rea** > **W-[2]-Rea** > **W-[1]-Rea**. This strongly implies that the singlet−triplet gap of the reactant becomes larger as one proceeds along the series from **M-[3]-Rea** to **M-Rea** to **M-[2]-Rea** to **M-[1]-Rea** (M = Mo and W), which has been confirmed by our DFT calculations as given in Table 1. Moreover, it is readily seen that this result is in accordance with the trend in activation energy and enthalpy (ΔE_{act}, ΔH) for Mo insertion, which are (3.60, −9.58), (5.50, −9.65), (10.1, −6.66), and (12.4, −5.11) kcal/mol, and for W insertion, which are (3.77, −26.4), (4.42, −23.7), (5.86, −22.4), and (5.49, −22.1) kcal/mol, respectively. Consequently, our model calculations provide strong evidence that the electronic factor resulting from the ansa-bridged structure should play a decisive role in determining the reactivity of [*n*]-metallocenophane.

(b) Why is the W reaction more favorable than the Mo reaction in the activation of the C−H bond?

The reason for this can also be simply understood in terms of the singlet−triplet gap (ΔE_{st}) of 16-electron [*n*]-metallocenophane. According to the experiments,[33] the Mo atom has a seventet d^5s^1 ground state with a high excitation energy of 31

kcal/mol to the quintet d^4s^2 state. For the W atom, the ground state is quintet d^4s^2 but with a relatively low excitation energy of 8.4 kcal/mol to the seventet d^5s^1 state. This implies that W would prefer to remain in a high-spin state, whereas Mo favors a low-spin state. In fact, our B3LYP/LANL2DZ results in Table 1 indicates that, for the same geometrical structure, ΔE_{st} of the W complex is generally smaller in energy than that of the Mo complex. This would lead to the fact that the insertion into a C−H bond should be more easier and more exothermic for the W system than for its Mo counterpart. This is what we observed in the 16-electron [*n*]-metallocenophane systems. Consequently, our theoretical findings are in good agreement with the CM model.

VI. Conclusion

As mentioned in the Introduction, in the traditional explanation, the reactivity of the ansa-bridged metallocene complex is attributed to its bent sandwich structure resulting in a hybridized HOMO (see $1b_2$ in Figure 1) that points away from the two Cp ligands and thus leads to a better overlap for the incoming hydrocarbon molecule. That is to say, using this conventional belief, one may predict that the oxidative addition reaction of [*n*]-metallocenophane with bent structure should be more facile than that of parallel ring sandwich complex. This is, however, contrary to many experimental findings.[10−16] Our study has shown that this conventional belief is refuted by a simple valence-bond model (i.e., the CM model), which help us understand the electronic origin of an activation barrier for addition of methane to 16-electron [*n*]-metallocenophane.

Despite the fact that the estimated magnitude of the barrier and the predicted geometry of the transition state for such reactions appear to be dependent on the computational level applied, our qualitative predictions are in good agreement with the computational results presented here as well as the experimental observations. Despite its simplicity, our approach proves to be rather effective and can provide chemists with important insights into the factors controlling the activation of saturated C−H bonds, thus allowing a better understanding of the nature of such systems as well as a number of predictions to be made.

Acknowledgment. We thank the National Center for High-Performance Computing of Taiwan and the Computing Center at Tsing Hua University for generous amounts of computing time and the National Science Council of Taiwan for their financial support. We are grateful to the reviewers for their critical comments and helpful corrections of the manuscript.

Appendix: Computational Details

All geometries were fully optimized without imposing any symmetry constraints, although in some instances the resulting structure showed various elements of symmetry. Furthermore, the transition states were characterized by normal-mode analysis to identify them as real transition states (one imaginary frequency) or second-order saddle points (two imaginary frequencies). The DFT calculations used the Becke hybrid functional (B3LYP)[34] as implemented in the GAUSSIAN94 program.[35]

Effective core potentials (ECP) were used to represent the 28 innermost electrons of molybdenum (up to the 3d shell).[36] Likewise, ECPs were used to represent the 60 innermost electrons of tungsten (up to the 4f shell).[37] For hydrogen, carbon, and oxygen atoms the double-ζ basis of Dunning−Huzinaga was used.[38] Moreover, the unrestricted B3LYP approach was used in this work to describe the triplet states of reactants. Hence, all the B3LYP calculations are denoted by B3LYP/LANL2DZ.[39]

References and Notes

(1) Janowicz, A. H.; Bergman, R. G. *J. Am. Chem. Soc*. **1982**, *104*, 352. (b) Janowicz, A. H.; Bergman, R. G. *J. Am. Chem. Soc*. **1983**, *105*, 3929.

(2) For reviews, see: (a) Parshall, G. W. *Acc. Chem. Res*. **1975**, *8*, 113. (b) Bergman, R. G. *Science* **1984**, *223*, 902. (c) Janowicz, A. H.; Perima, R. A.; Buchanan, J. M.; Kovac, C. A.; Struker, J. M.; Wax, M. J.; Bergman, R. G. *Pure Appl. Chem*. **1984**, *56*, 13. (d) Hill, C. L. *Activation and Functionalization of Alkanes*; Wiley: New Tork, 1989. (e) Halpern, J. *Inorg. Chim. Acta* **1985**, *100*, 41. (f) Ephritikhine, M. *New J. Chem*. **1986**, *10*, 9. (g) Jones, W. D.; Feher, F. J. *Acc. Chem. Res*. **1989**, *22*, 91. (h) Ryabov, A. D. *Chem. Rev*. **1990**, *90*, 403. (i) Davies, J. A.; Watson, P. L.; Liebman, J. F.; Greenberg, A. *Selective Hydrocarbon Activation, Principles and Progress*; VCH Publishers, Inc.: New York, 1990. (j) Bergman, R. G. *J. Organomet. Chem*. **1990**, *400*, 273. (k) Koga, N.; Morokuma, K. *Chem. Rev*. **1991**, *91*, 823. (l) Ziegler, T. *Chem. Rev*. **1991**, *91*, 651. (m) Bergman, R. G. *Adv. Chem. Series* **1992**, *230*, 211. (n) Wasserman, E. P.; Moore, C. B.; Bergman, R. G. *Science* **1992**, *255*, 315. (o) Crabtree, R. H. *Angew. Chem., Int. Ed. Engl*. **1993**, *32*, 789. (p) Schroder, D.; Schwarz, H. *Angew. Chem., Int. Ed. Engl*. **1995**, *34*, 1937. (q) Lees, A. J.; Purwoko, A. A. *Coord. Chem. Rev*. **1994**, *132*, 155. (r) Amdtsen, B. A.; Bergman, R. G.; Mobley, T. A.; Peterson, T. H. *Acc. Chem. Res*. **1995**, *28*, 154. (s) Ziegler, T. *Can. J. Chem*. **1995**, *73*, 743. (t) Arndtsen, B. A.; Bergman, R. G. *Science* **1995**, *270*, 1970. (u) Lohrenz, J. C.; Jacobsen, H. *Angew. Chem., Int. Ed. Engl*. **1996**, *35*, 1305.

(3) (a) Niu, S.; Hall, M. B. *Chem. Rev*. **2000**, *100*, 353. (b) Siegbahn, P. E. M.; Blomberg, R. A. *Chem. Rev*. **2000**, *100*, 421.

(4) Saillard, J. Y.; Hoffmann, R. *J. Am. Chem. Soc.* **1984**, *106*, 2006.

(5) Dedieu, A. *Chem. Rev*. **2000**, *100*, 543.

(6) (a) Torrent, M.; Sola, M.; Frenking, G. *Chem. Rev*. **2000**, *100*, 439. (b) Frenking, G.; Frohlich, N. *Chem. Rev*. **2000**, *100*, 717.

(7) (a) Loew, G. H.; Harris, D. L. *Chem. Rev*. **2000**, *100*, 407. (b) Alonso, J. A. *Chem. Rev*. **2000**, *100*, 637. (c) Harrison, J. F. *Chem. Rev*. **2000**, *100*, 679.

(8) Green, J. C. *Chem. Soc. Rev*. **1998**, *27*, 263.

(9) The term ansa (meaning bent handle, attached at both hands) was first introduced with respect to metallocene chemistry by Brintzinger. See: Smith, J. A.; von Seyerl, J.; Huttner, G.; Brintzinger, H. H. *J. Organomet. Chem*. **1979**, *173*, 175.

(10) For recent reviews, see: (a) Nguyen, P.; Gomez-Elipe, P.; Manners, I. *Chem. Rev*. **1999**, *99*, 1515. (b) Hoveyda, A. H.; Morken, J. P. *Angew. Chem., Int. Ed. Engl*. **1996**, *35*, 1262.

(11) Green, M. L. H.; O'Hare, D. *Pure Appl. Chem*. **1985**, *57*, 47 and references therein.

(12) (a) Labella, L.; Chernega, A.; Green. M. L. H. *J. Chem. Soc., Dalton Trans*. **1995**, 395. (b) Labella, L.; Chernega, A.; Green. M. L. H. *J. Organomet. Chem*. **1995**, *485*, C18−C21.

(13) (a) Grebenik, M.; Downs, A. J.; Green, M. L. H.; Perutz, R. N. *J. Chem. Soc., Chem. Commun*. **1979**, 742. (b) Chetwynd-Talbot, J.; Grebnik, P.; Perutz, R. N. *Inorg. Chem*. **1982**, *21*, 3647. (c) Cox, P. A.; Grebenik, P.; Perutz, R. N.; Robinson, M. D.; Grinter, R.; Stern, D. R. *Inorg. Chem*. **1983**, *22*, 3614.

(14) (a) Gianotti, C.; Green, M. L. H. *J. Chem. Soc., Chem. Commun*. **1972**, 1114. (b) Cooper, N. J.; Green, M. L. H.; Mahtab, R. *J. Chem. Soc., Dalton Trans*. **1979**, 1557. (c) Berry, M.; Elmitt, K.; Green, M. L. H. *J. Chem. Soc., Dalton Trans*. **1979**, 1950. (d) Berry, M.; Cooper, N. J.; Green, M. L. H.; Simpson, S. J. *J. Chem. Soc., Dalton Trans*. **1980**, 29. (e) Canestrari, M.; Green, M. L. H. *Polyhedron* **1982**, *1*, 629. (f) Green, M. L. H. *Pure Appl. Chem*. **1984**, *56*, 47.

(15) Green, J.; Jardine, C. N. *J. Chem. Soc., Dalton Trans*. **1998**, 1057.

(16) (a) Conway, S. L. J.; Dijkstra, T.; Doerrer, L. H.; Green, J. C.; Green, M. L. H.; Stephens, A. H. H. *J. Chem. Soc., Dalton Trans*. **1998**, 2689. (b) Cherenga, A.; Cook, J.; Green, M. L. H.; Labella, L.; Simpson, S. J.; Souter, J.; Stephens, A. H. H. *J. Chem. Soc., Dalton Trans*. **1997**, 3225.

(17) Albright, T. A.; Burdett, J. K.; Whangbo, M. H. *Orbital Interaction in Chemistry*; Wiley: New York, 1985; p 394.

(18) (a) Recently, Green and Jardine have used DFT with STO-3G plus some polarization functions to study the hydrogen exchange and methane elimination reactions of $[W(\eta\text{-}C_5H_5)_2(Me)H]$ and $[W\{\eta\text{-}C_5H_4)_2CH_2\}(Me)H]$. For more details, see ref 15. (b) It has been demonstrated in ref 15 that the relative singlet−triplet energies in the two species are crucial in determining their relative stabilities.

(19) (a) Green, J. C.; Jardine, C. N. *J. Chem. Soc., Dalton Trans*. **1999**, 3767. (b) Green, J. C.; Scottow, A. *New J. Chem*. **1999**, *23*, 651.

(20) Lauher, J. W.; Hoffmann, R. *J. Am. Chem. Soc*. **1976**, *98*, 1729.

(21) Ziegler, T.; Cheng, W.; Baerends, E. J.; Ravenek, W. *Inorg. Chem*. **1988**, *27*, 3458.

(22) (a) McGlynn, S. P.; Azumi, T.; Kinoshita, M. *The Triplet State*; Prentice-Hall: New York, 1969; pp 190−198. (b) El-Sayed. M. A. *J. Phys. Chem*. **1963**, *38*, 2834. (c) El-Sayed, M. A. *Acc. Chem. Res.* **1968**, *1*, 8.

(23) (a) Su, M.-D. *Chem. Phys. Lett.* **1995**, *237*, 317. (b) Su, M.-D. *J. Org. Chem*. **1995**, *60*, 6621. (c) Su, M.-D. *J. Phys. Chem*. **1996**, *100*, 4339. (d) Su, M.-D. *Chem. Phys*. **1996**, *205*, 277. (e) Su, M.-D. *J. Org. Chem*. **1996**, *61*, 3080.

(24) Suppose the formation of the σ-complex is at the triplet state; this means that it contains 18-electron at the triplet state. Therefore, one electron must go to the antibonding d orbital, which makes the σ-complex itself unstable and then easily get apart. Moreover, as far as we know the calculations about the σ-complex in ref 15, they did not fully optimized the triplet σ-complex, which made their statement doubtful. Indeed, we tried every possibility to fully optimized the triplet σ-complex using different theoretical methods but always failed. Therefore, we had calculated the single-point calculation for the triplet σ-complex using its singlet geometry, and we found that its energy is quite high (about 54 kcal/mol at the B3LYP/LANL2DZ level) compared to the singlet σ-complex. For these reasons, we believe that the oxidative addition reactions proceed on the singlet surface before the triplet σ-complex is formed. Consequently, it is reasonable to focus on the singlet surface.

(25) Su, M.-D.; Chu, S.-Y. *J. Am. Chem. Soc.* **1997**, *119*, 5373.

(26) (a) Su, M.-D.; Chu, S.-Y. *Chem. Phys. Lett*. **1998**, *282*, 25. (b) Su, M.-D.; Chu, S.-Y. *Organometallics* **1997**, *16*, 1621. (c) Su, M.-D.; Chu, S.-Y. *J. Phys. Chem.* **1997**, *101*, 6798. (d) Su, M.-D.; Chu, S.-Y. *Eur. J. Chem*. **1999**, *5*, 198.

(27) Su, M.-D.; Chu, S.-Y. *J. Phys. Chem.* **1998**, *102*, 10159.

(28) Su, M.-D.; Chu, S.-Y. *Inorg. Chem.* **1998**, *37*, 3400 and references therein.

(29) Bullock, R. M.; Headford, C. E. L.; Hennessy, K. M.; Kegley, S. E.; Norton, J. R. *J. Am. Chem. Soc.* **1989**, *111*, 3897.

(30) Parkin, G.; Bercaw, J. E. *Organometallics* **1989**, *8*, 1172.

(31) (a) Shaik, S. *J. Am. Chem. Soc*. **1981**, *103*, 3691. (b) Shaik, S.; Schlegel, H. B.; Wolfe, S. *Theoretical Aspects of Physical Organic Chemistry*; John Wiley & Sons Inc.: New York, 1992. (c) Pross, A. *Theoretical and Physical Principles of Organic Reactivity*; John Wiley & Sons Inc. New York, 1995.

(32) Su, M.-D. *Inorg. Chem*. **1995**, *34*, 3829.

(33) Moore, C. E. *Atomic Energy Levels*; NBS: Washington, DC, 1971; Vol. III.

(34) (a) Becke, A. D. *Phys. Rev. A* **1988**, *38*, 3098. (b) Lee, C.; Yang, W.; Parr, R. G. *Phys. Rev. B* **1988**, *37*, 785. (c) Becke, A. D. *J. Chem. Phys*. **1993**, *98*, 5648.

(35) Frisch, M. J.; Trucks, G. W.; Schlegel, H. B.; Gill, P. M. W.; Johnson, B. G.; Robb, M. A.; Cheeseman, J. R.; Keith, T.; Petersson, G. A.; Montgomery, J. A.; Raghavachari, K.; Al-Laham, M. A.; Zakrzewski, V. G.; Ortiz, J. V.; Foresman, J. B.; Cioslowski, J.; Stefanov, B. B.; Nanayakkara, A.; Challacombe, M.; Peng, C. Y.; Ayala, P. Y.; Chen, W.; Wong, M. W.; Andres, J. L.; Replogle, E. S.; Gomperts, R.; Martin, R. L.; Fox, D. J.; Binkley, J. S.; Defrees, D. J.; Baker, J.; Stewart, J. P.; Head-Gordon, M.; Gonzalez, C.; Pople, J. A. *Gaussian 94*; Gaussian, Inc.: Pittsburgh, PA, 1995.

(36) Hay, J. P.; Wadt, W. R. *J. Chem. Phys*. **1985**, *82*, 299.

(37) Hay, J. P.; Wadt, W. R. *J. Chem. Phys*. **1985**, *82*, 284.

(38) Dunning, T. H.; Hay, P. J. In *Modern Theoretical Chemistry*; Schaefer, H. F., Ed., Plenum: New York, 1976; pp 1−28.

(39) It has to be emphasized that calculated DFT barrier heights are often, if anything, too low; see: *Chemical Applications of Density Functional Theory*; Laird, A., Ross, R. B., Ziegler, T., Eds.; American Chemical Society: Washington, DC, 1996. Thus, those barrier numbers might be underestimated by down to several kilocalories per mole. It is believed that using the more sphosticipated theory with larger basis sets should be essential. Nevertheless, the energies obtained at the B3LYP/LANL2DZ level can, at least, provide the reliably qualitative conclusions.